



MECHANICAL ANCHORAGE OF MAIN BARS IN BEAM-COLUMN JOINTS

MASAHIDE MURAKAMI and TOSHIYUKI KUBOTA

Department of Architecture, Faculty of Science & Technology, KINKI University
3-4-1 Kowakae, Higashi-Osaka, Osaka, JAPAN, 577

ABSTRACT

Screw type rolled bars have become popular to use as reinforcing bars for reinforced concrete structures. The mechanical anchorage device which consists of nut with small flange is already developed in Japan. It becomes easier to connect an anchorage device to a longitudinal reinforcement with frictional welding. The mechanical anchorage has the more advantage of arrangement of longitudinal bars in beam-column joints than 90-deg. hooked bar anchorage, especially for high strength steel bars whose bending works are difficult.

Though there is the design concept of the mechanical anchorage on prestressed concrete structures in many countries, that on longitudinal bars in beam-column joints of reinforced concrete structures is not established yet. Ninety eight pull-out tests and 14 subassemblage frame tests have already been carried out to investigate the load carrying capacity of mechanical anchorages and ductility of beam-column joints with mechanical anchorages.

The anchorage capacity and failure behavior of external joint panels are discussed based on 56 pull out tests and 12 subassemblage frame tests. The conclusions are obtained as follows;

- 1) The ultimate strength of anchorage is estimated based on pull-out test results. The anchorage capacity of mechanical anchorages can be predicted by suggested Equation.
- 2) The load carrying capacity and ductility of beam-column joints with mechanical anchorages under three failure types (flexural yielding of a beam, shear failure of a joint, and side splitting failure of concrete cover around anchorage) are discussed by comparing with those with 90-deg. hooked bar anchorages based on frame test results. The physical performance of mechanical anchorages is approximately equal to one of 90-deg. hooked bar anchorages.

KEYWORDS

mechanical anchorage; external beam-column joint; anchorage capacity; reinforced concrete structure; ductility

MECHANICAL ANCHORAGE OF MAIN BARS IN BEAM-COLUMN JOINTS

MASAHIDE MURAKAMI and TOSHIYUKI KUBOTA

Department of Architecture, Faculty of Science & Technology, KINKI University
3-4-1 Kowakae, Higashi-Osaka, Osaka, JAPAN, 577

ABSTRACT

Though there is the design concept of the mechanical anchorage on prestressed concrete structures in many countries, that on longitudinal bars in beam-column joints of reinforced concrete structures is not established yet. Ninety eight pull-out tests and 14 subassemblage frame tests have already been carried out to investigate the load carrying capacity of mechanical anchorages and ductility of beam-column joints with mechanical anchorages.

Two topics are discussed based on essential test results in this paper;

- 1) The ultimate strength of anchorage is estimated based on pull-out test results.
- 2) The load carrying capacity and ductility of beam-column joints with mechanical anchorages under three failure types (flexural yielding of beams, shear failure of joint panels, and side splitting failure of concrete cover around anchorage) are discussed by comparing with those with 90-deg. hooked bar anchorages based on frame test results.

KEYWORDS

mechanical anchorage; external beam-column joint; anchorage capacity; reinforced concrete structure; ductility

INTRODUCTION

Screw type rolled bars have become popular to use as reinforcing bars for reinforced concrete structures. The mechanical anchorage device which consists of nut with small flange is already developed in Japan. It becomes easier to connect an anchorage device to a longitudinal reinforcement with frictional welding. The mechanical anchorage has the more advantage of arrangement of longitudinal bars in beam-column joints than 90-deg. hooked bar anchorage, especially for high strength steel bars whose bending works are difficult.

Though the design concept of the mechanical anchorage on prestressed concrete structures has already established in many countries, that of longitudinal bars in beam-column joints of reinforced concrete structures is not established yet in any country. To establish the design concept of the mechanical anchorage in external beam-column joints, 98 pull-out tests and 14 subassemblage frame tests have already been carried out by authors. The essential test results to establish the design concept are discussed in this paper.

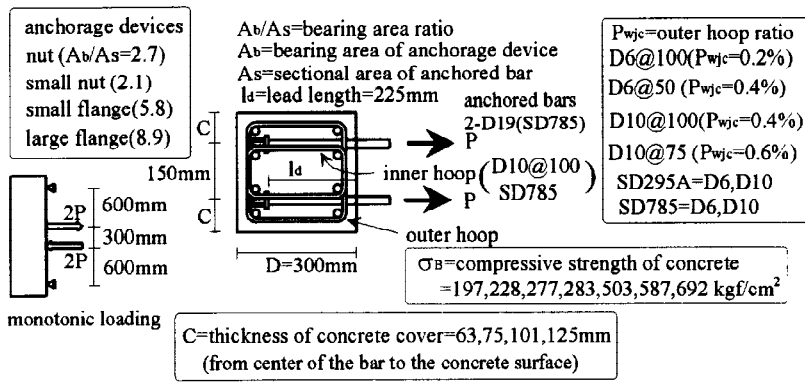


Fig. 1. Experimental parameters to estimate anchorage capacities (Series A)

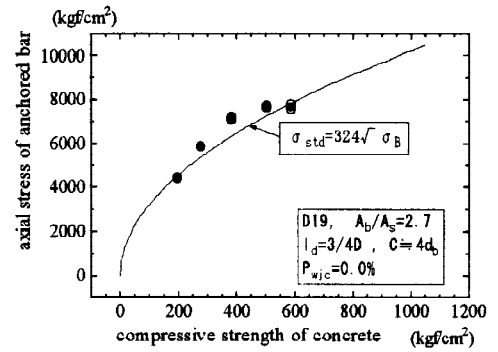


Fig. 2. Effect of compressive strength of concrete

ESTIMATION OF ANCHORAGE CAPACITY

To estimate the mechanical anchorage capacity in the external beam-column joint, the 46 pull out tests were carried out. The specimens and their experimental parameters are shown in Fig.1. The specimens represent the external beam-column joints without beams. The high strength screw type rolled bars were used as the longitudinal reinforcements of beams. The anchorage capacity of arbitrary specimens is assumed to be estimated by multiplying the modification factors to those of the standard specimens as shown in Eq.1. Three modification factors were introduced and determined by regression analyses based on experimental data.

$$\sigma = k_1 k_2 k_3 \sigma_{std} \quad (1)$$

where σ : anchorage capacity (stress of an anchored bar)
 k_1 : modification factor on bearing area ratio
 k_2 : modification factor on thickness of concrete cover
 k_3 : modification factor on transverse reinforcements (outer hoops) in concrete cover
 σ_{std} : anchorage capacity (stress) of standard specimens

The Effect of Concrete Strength

The anchorage capacity of standard specimens is given in Eq.2 which is determined by the curve fitting method of a square root function as shown in Fig.2.

$$\sigma_{std} = 324 \sqrt{\sigma_B} \quad (2)$$

where σ_B : compressive strength of concrete (kgf/cm²)

In this figure, the anchorage capacities of the standard specimens with several kinds of concrete strengths were plotted. The details of the standard specimens are;

- 1) The bearing area of the mechanical anchorage device is equal to 2.7 times of cross sectional area of the anchored bar. (Nuts without flanges are used as anchorage devices)
- 2) The lead length of anchorage l_d is equal to $3/4D$ (D : depth of the column) of the column.
- 3) The thickness of concrete cover (from the concrete surface to center of the anchored bar) is 4 times as much as the longitudinal bar diameter.
- 4) No transverse reinforcement (outer hoop) is arranged in concrete cover.

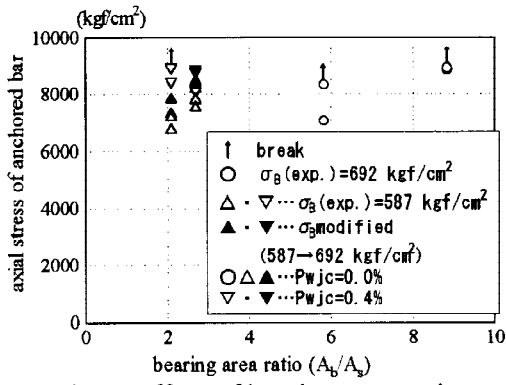


Fig. 3. Effect of bearing area ratio

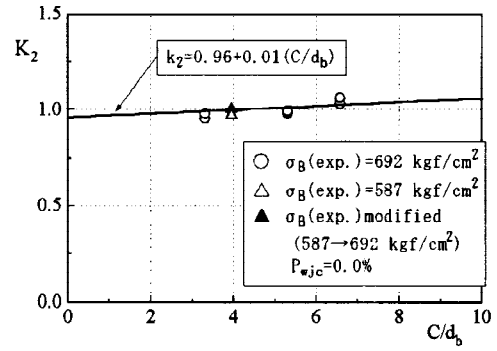


Fig. 4. Effect of concrete cover thickness

The Effect of Bearing Area Ratio

Fig.3 shows the effect of bearing area ratio under outer hoop ratio $P_{wjc}=0\%$ or 0.4% ($P_{wjc}=a_s/bx$, a_s is the area of a set of outer hoop arranged in concrete cover, b is the width of a column, x is the pitch of outer hoops). The original data, whose concrete strengths are $\sigma_B=587$ and 692 kgf/cm², are plotted with white markers in this figure. The black ones indicate the modified values from $\sigma_B=587$ kgf/cm² to 692 kgf/cm² by Eq.2.

The anchorage capacities are approximately same values regardless of bearing area ratio under same confinement conditions (i.e. thickness of concrete cover and outer hoop ratio). Herein the modification factor k_1 is assumed to be equal to 1.0.

The Effect of Concrete Cover Thickness

The anchorage capacities of 4 specimens which have different concrete cover thickness without outer hoop are shown in Fig.4. The white marks indicate original data and/or the black ones indicate modified ones mentioned above. The modification factor k_2 against the specimens with standard thickness ($C=4d_b$, d_b : anchored bar diameter) slightly increases with the increase of concrete cover thickness.

The Effect of Outer Hoop Ratio

The effect of hoops in concrete cover is investigated on two concrete batches ($\sigma_B=277$ kgf/cm² and $\sigma_B=587$ kgf/cm²). The the modification factor k_3 against $P_{wjc}=0\%$ under each batch are plotted in Fig.5(a) and (b) respectively. The upper limits of the effect of outer hoop are detected when $P_{wjc}>0.4\%$. It seems to be dominated not by the yielding strengths of outer hoop but by the amount of hoops in concrete cover. The upper limit of capacity when $P_{wjc}>0.4\%$ is 1.25 times as much as the capacity when $P_{wjc}=0\%$ under $\sigma_B=277$ kgf/cm² and 1.10 times as much as that under $\sigma_B=587$ kgf/cm².

In case of 277kgf/cm²

$$k3'=62.5P_{wjc}+1 \quad (\text{when } P_{wjc} \leq 0.4\%) \quad k3'=1.25 \quad (\text{when } P_{wjc} > 0.4\%) \quad (3)$$

In case of 587kgf/cm²

$$k3''=25P_{wjc}+1 \quad (\text{when } P_{wjc} \leq 0.4\%) \quad k3''=1.10 \quad (\text{when } P_{wjc} > 0.4\%) \quad (3')$$

Verifications

The modification factors k_1 and k_2 are approximately constant values (=1.0). Herein only k_3 is considered

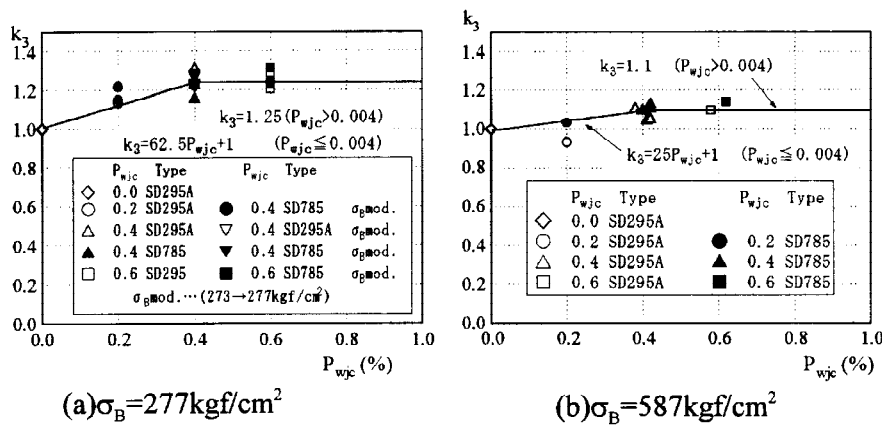


Fig. 5. Effect of outer hoop ratio

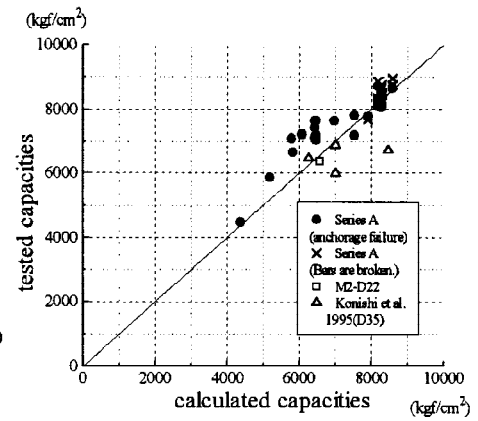


Fig. 6. Verifications

in Eq. 1. Substituting Eq. 2 and 3 to Eq. 1, Eq. 4 are obtained;

$$\sigma = k_3 324 \sqrt{\sigma_B} \quad (4)$$

where k_3 is the modification factor of outer hoop in concrete cover which is calculated by the linear interpolation between Eq. (3) and Eq. (3') as written in Eq. 5.

$$k_3 = k_3' - (k_3' - k_3'')(\sigma_B - 277) / 310 \quad (5)$$

Fig. 6 shows the comparisons between calculated and tested anchorage capacities of 23 specimens failed by anchorages. The black marks indicate the "series A" specimens with D-19 anchored bars with anchorage failure which are used to establish Eqs. 1-5, and/or the marks "X" indicate those with broken bars. The white ones indicate M2-dD22 (see later) and/or the 4 specimens tested in other institute in Japan. The mean value of capacity ratio (tested/calculated) is equal to 1.04 and the coefficient of variation is equal to 0.01. It remarks that the calculated/tested capacity ratio is equal to 0.91, in case of large size anchored bars (D-35, Konishi *et al.* 1995).

SUBASSEMBLAGE FRAME TESTS

Ten specimens which represent external frames (T type) were tested to investigate the interaction between anchorage failure, shear failure of joint panels and flexural yielding of beam ends. The specifications of specimens are shown in Fig. 7 and Table 1. The tested and calculated capacities and failure modes etc. are also written in Table 2. The relative displacements between anchorage devices and adjacent concrete core (pull out displacement) were also measured in M4-D19, M3-D19, and M2-D22 as shown in Fig. 8. All specimens were loaded under the cyclic loading program. Nuts with small flanges, whose diameters ($\phi = 2.5db$) are less than the minimum spacing of steel bars required in the Japanese building code, were used as anchorage devices in the subassembly tests. It is quantitatively difficult to distinguish between anchorage failure and shear failure of joint panels. Herein the anchorage failure mode is judged by comparing various informations such as cracking pattern, expansion of concrete cover, pull out displacements of anchorage devices, plastic strains of hoops and etc. with those of specimens failed by shear in joint panels.

Shear Failure Type Specimens

To investigate the interaction between anchorage failure and shear failure of joint panels, 4 specimens which had different amount of longitudinal bars of beams were tested. All specimens were failed by shear in joint panels, because the high strength steel bars were used as longitudinal bars of beams. The load-displacement

curves at loading points are illustrated in Fig. 9.

The pull out displacements at the anchorage devices are shown in Table 3. The pull out displacements become larger with reduction of tensile reinforcement area (a_s) of beams (M4-D19>M3-D19> M2-D22, note that the pull out displacements of M8-D16 are not compared with ones of other specimens directly, because displacement δ_2 in Fig.8 was not measured in M8-D16), and the peak load carrying capacities becomes smaller in the same order. The plastic strains of hoops in joint panels are 10000μ in M4-D19, 9000μ in M8-D16, 6000μ in M3-D19, and 3000μ in M2-D22. It was observed in M2-D22 that the concrete cover split and expanded out of surface of the joint panel clearly and it was not observed in M8-D16 and M4-D19 at all. The failure mode of each specimen is judged as follows; the peak capacity of M2-D22 is dominated by anchorage failure, and/or that of M8-D16 is dominated by shear failure of the joint panel. The Peak capacities of M4-D19 and M3-D19 are dominated by shear failure in the joint panels because pull out displacements of both specimens were smaller than one of M2-D22 when $R=1/50$ rad. (at the peak capacity). The load carrying capacity of M3-D19 when $R>1/25$ rad. seems to be dominated by anchorage failure, because it drops more than one of M4-D19 and that the pull out displacement of M3-D19 is larger than one of M4-D19 at $R=1/25$ rad.

Flexural Yielding Type Specimens

No.100 and 101 specimens with flexural yielding of beam ends which have different bearing area ratio each other were tested. The load-displacement curves are shown in Fig.10(a) and (b). The bearing area ratios of No.100 and 101 are equal to 1.7 and 6.3 respectively.

Both specimens behave as flexural yielding failure mode until $R=1/25$ rad. The load carrying capacity of No.100 deteriorates after the cyclic deformation of $R=1/25$ rad., because the pull out displacement of the anchorage device increases as shown in Table 4(a). The confinement surround the small anchorage device (a small nut without flange) decrease because the diameter of bars becomes smaller due to the plastic elongation under large cyclic deformation in No.100.

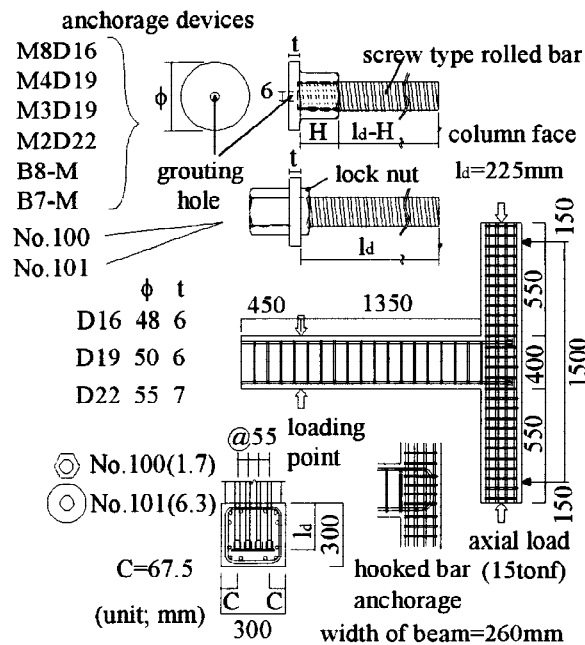


Fig. 7. Subassembly frame tests(Series B)

Table 1. Material of subassemblage frames

specimen	longitudinal bars			transverse bars			concret σ_B	type	$\frac{A_b}{A_s}$
	tensile bars	σ_y	σ_{max}	outer hoop ratio	σ_y	σ_{max}			
No.100								M-N	1.7
No.101	4-D16	3770	7130	0.48%	3870	5490	401	M-F	6.3
B8-M				0.73	3750	5300	301	M-F	6
B8-U	3-D19	5210	7010					H	---
B7-M	2-D19	5210	7010					M-F	6
B7-U	1-D16	3820	5560					H	---
No.102								M-N	2.1
No.103								M-F	5.8
No.104	4-D19	9640	11120	0.73	3870	5490	401	M-P	13.4
No.105								H	---
M8D16	8-D16			0.73	3750	5300	288	M-F	6.0
M4D19	4-D19	10200	11700						
M3D19	3-D19								
M2D22	2-D22	10200	11400						

unit: kgf/cm²

anchorage device type M-N=nut, M-F=nut with flange
M-P=anchor plate, H=90-deg. hook

To compare with the physical performance of mechanical anchorages and one of 90-deg. hooked bar anchorages, two sets of specimens which were failed by flexural yielding at the beam ends were tested. The

peak shear stresses in their joint panels when yielding by flexure of the beams were designed to be approximately equal to 70% or 80% of their shear strengths which were predicted by the experimental result of M4-D19 and/or M3-D19 (actually peak shear stresses of joint panels were 87% and 77%, respectively). The load-displacement curves are shown in Fig.10(c)(d)(e) and (f). The pull out displacements are shown in Table 4(b). All specimens also behave as flexural yielding failure mode until R=1/25rad. The load carrying capacities of all specimens deteriorate after the cyclic deformation of R=1/25rad. due to the anchorage failure. Though the pull out displacements of mechanical anchorages at R=1/25rad. are larger than ones of 90-deg. hooked bar anchorages as shown in Table 4(b), the load carrying capacities of mechanical anchorages after R=1/25rad. are slightly larger than ones of 90-deg. hooked bar anchorages. In practice, it is concluded that the physical performance of mechanical anchorages is approximately equal to one of 90-deg. hooked bar anchorages.

Table 2. Subassemblage frame test results

Specimen No.		100	101	B8-M	B8-U	B7-M	B7-U	M8D16	M4D19	M3D19	M2D22	
failure mode	at peak	F	F	F	F	F	F	S	S	S	A	
	at ultimate	S	F	S	A	A	A	S	S	A	A	
experimental	maximum shear force of beam Qmax(tonf)	Pos.	8.8	9.1	11.9	12.1	10.6	10.3	15.3	14.4	14.3	11.3
		Neg.	8.8	10.1	11.9	11.0	10.6	9.9	14.8	12.9	13.0	10.9
		Ave.	8.8	9.6	11.9	11.6	10.6	10.1	15.1	13.7	13.7	11.1
	max. shear force in joint panel Qj(tonf)	Pos.	29.5	30.5	39.9	40.6	35.6	34.6	51.3	48.3	48.0	37.9
		Neg.	29.5	33.9	39.9	36.9	35.6	33.2	49.7	43.3	43.6	36.6
		Ave.	29.5	32.2	39.9	38.8	35.6	33.9	50.5	45.8	45.8	37.2
	τ_j (Qj/be.Ld) (kgf/cm ²)	Pos.	46.9	48.5	63.4	64.4	56.5	54.9	81.5	76.7	76.2	60.2
		Neg.	46.9	53.8	63.4	58.6	56.5	52.7	78.8	68.7	69.2	58.0
		Ave.	46.9	51.1	63.4	61.5	56.5	53.8	80.1	72.7	72.7	59.1
	τ_j' (Qj/be.Ld1) for Teraoka's	Pos.	53.9	55.8	72.9	74.2	65.0	63.2	101.0	88.3	87.6	69.3
		Neg.	53.9	61.9	72.9	67.4	65.0	60.2	97.7	79.1	79.7	66.8
		Ave.	53.9	58.8	72.9	70.8	65.0	61.9	99.3	83.7	83.7	68.0
	Pamax(tonf)		9.4	10.8	17.3	16.3	15.4	14.6	8.3	15.7	20.8	24.6
	Qby(tonf)		7.2	7.2	10.4	10.4	8.7	8.7	37.9	27.3	20.5	17.9
	Pa(tonf)		14.8	14.8	20.1	*14.8	20.1	*14.8	13.3	19.2	19.2	25.9
calculated	τ_j	Teraoka <i>et al.</i> 1992	61.4		57.2		54.0		84.7	66.4	56.5	51.6
		AIJ	63.8		47.9				45.8			
		ACI	63.7		55.2				54.0			

F=flexural yield at beam end, S=shear failure in joint panel, A=anchorage failure,
Pamax=tested maximum axial forces of an anchored bar, Pa=calculated anchorage capacity
Qby=calculated shear force by flexural yielding of beam end
be=averaged width of joint panel=(width of column+width of beam)/2
Teraoka's Eq. $\tau_j' = 1.32 \cdot \sigma_B^{0.46} \cdot P_t^{0.66} \cdot (l_d/d_b)^{0.28} \cdot (Ld_1 + j_b) / \sqrt{(Ld_1^2 + j_b^2)} + 0.4 \cdot P_w \cdot \sigma_y$
 σ_B =compressive strength of concrete(kgf/cm²), P_t =tensile reinforcement ratio of beam(%)
 d_b =longitudinal bar diameter of beam (mm), P_w =hoop ratio of joint panel (not in %)
 σ_y =yield point of hoop(kgf/cm²)

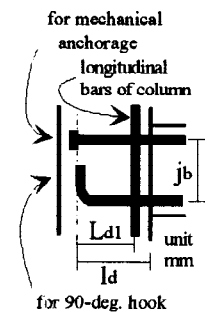
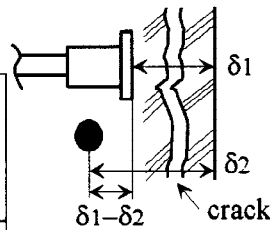


Table 3. Pull out displacements of shear failure type specimens

bar arrangements				
specimen	M4D19	M3D19	M2D22	
at(cm ²)	11.5	8.6	7.7	
position	A	B	A	
R	1/400	0.0	0.0	0.0
	1/200	0.1	0.1	0.7
	1/100	0.2	0.3	0.2
	1/50	0.6	0.7	0.0
	1/25	1.0	1.7	2.9

bar arrangement				
specimen	M8D16			
at(cm ²)	15.9			
position	A	B	C	D
R	1/400	0	0.4	0.1
	1/200	0.1	0.2	0.2
	1/100	0.6	0.7	0.7
	1/50	2.4	2.5	2.9
	1/25	4.7	5.6	9.5



The pull out displacement is measured as follows;
 $\delta_1 - \delta_2$ is used in M4D19, M3D19, M2D22.
 δ_1 is used in other specimens.

Fig. 8. Measurement of pull out displacement

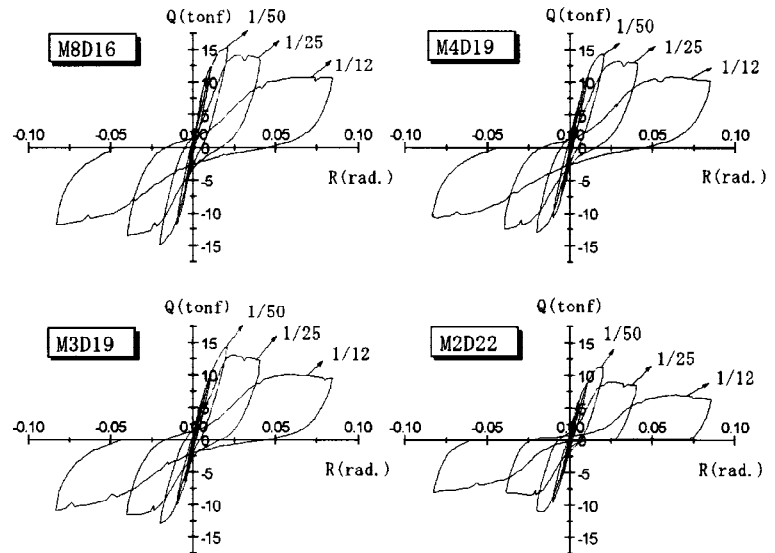


Fig. 9. Load-displacement curves of shear failure type specimens

Table 4. Pull out displacements of flexural yielding type specimens

(a) effect of bearing area ratio

bar arrangement			
specimen	No.100	No.101	
Ab/As	1.7	6.3	
position	A	A	
R	1/400	0.0	0.0
	1/200	----	0.0
	1/200	----	----
	1/100	0.2	0.2
	1/100	0.3	0.3
	1/50	0.6	0.5
	1/25	1.5	0.5

(b) mechanical v.s. 90-deg hooked anchorages

bar arrangement					
specimen	B7-M		B8-M		
position	A	B	A	B	
R	1/400	----	----	----	
	1/200	0.3	----	0.2	0.2
	1/100	0.7	0.4	0.7	0.6
	1/50	1.1	0.7	1.2	1.2
	1/25	1.8	1.5	2	3.3
specimen	B7-U		B8-U		
position	A	B	A	B	
R	1/400	0	0	0	
	1/200	0	----	0	----
	1/100	0.2	0.1	0.3	0.2
	1/50	0.3	0.2	0.6	0.4
	1/25	0.4	1.2	1.1	4.3